Mechanical Engineering Advances 2023; 1(1): 132.
Original Research Article

Thermal and viscous irreversibilities in the heat exchanger of individually finned heat pipes using freon R404A as the working fluid

Élcio Nogueira

Department of Mechanic and Energy, State University of Rio de Janeiro, Resende 27537-000, Rio de Janeiro, Brazil; elcionogueira@hotmail.com

ARTICLE INFO

Received: 1 September 2023
Accepted: 10 October 2023
Available online: 18 October 2023

doi: 10.59400/mea.v1i1.132

Copyright © 2023 Author(s).

Journal of AppliedMath is published by Academic Publishing Pte. Ltd. This article is licensed under the Creative Commons Attribution License (CC BY 4.0). https://creativecommons.org/licenses/by/4.0/

ABSTRACT: This work aims to apply a theoretical procedure to determine the performance of the heat exchanger of individually finned heat pipes used in an air conditioning system. The relevant physical quantities are defined and specified locally in the evaporator and condenser sections. The results obtained in the sections are associated with the theoretical determination of the global performance of the heat exchanger. Global theoretical results are compared with global experimental results. Thermal effectiveness, heat transfer rate, pressure drop, thermal and viscous irreversibilities, and thermodynamic Bejan number are determined at the evaporator, condenser, and heat exchanger. The relevant variables used to determine the results are the number of fins per heat pipe and rows of heat pipes. The theoretical-experimental comparison demonstrates that the localized model applied in the analysis is consistent and can be used as a design and comprehensive analysis tool for finessed heat exchangers. The performance of the heat exchanger demonstrated exceptionalness when comparing irreversibilities through the Bejan number, indicating a favorable cost-benefit ratio for the fins less than 30 and the number of heat pipes equal to 49. Bejan's thermodynamic number, which uses results related to thermal and viscous irreversibilities, demonstrated that one should look for the relationship between thermal irreversibility versus total irreversibility and that fin numbers between 10 and 20 for heat pipes equal to 49 provide a better cost-benefit ratio. The absolute percentage errors obtained between theoretical and experimental values, for an experimental number of fins equal to 30, for the overall heat transfer rate and overall thermal effectiveness range from 2.0% to 42.1%.

KEYWORDS: heat exchanger; individually finned heat pipe; air conditioning; freon R404A; thermal irreversibility; viscous irreversibility

1. Introduction

This work aims to apply the theory of thermal efficiency, based on the fin analogy and the second law of thermodynamics, to determine quantities of practical interest related to finned heat tube heat exchangers. The pioneering method advocated was initially applied locally in the evaporator and condenser. The results obtained locally were used for theoretical-experimental comparison using global experimental results obtained for the heat exchanger under analysis[1].

The heat exchanger under analysis consisted of individually finned heat pipes and was taken from theoretical-experimental work, presented through reference[1]. The apparatus was designed so that the configuration of the heat pipes is in a staggered formation. The number of heat pipes ranges from 7 to 49, and the number of rows from 3 to 21. The number of fins per heat pipe ranges from 0 to 40 in the theoretical model.

Górecki et al.[1] perform modeling and present an experimental study on a heat exchanger used as energy recovery in small air conditioning systems composed of individually finned heat pipes and R404A refrigerant as the working fluid. Parametric calculations were performed, and it was concluded that 20 rows of finned heat pipes in the staggered arrangement guarantee efficiency close to 60%. The experimental results showed a good level of agreement with the developed model. The heat pipes used in the experiments are 1 mm thick copper tubes with an external diameter of 20 mm and aluminum fins. They used a computational model to obtain heat transfer rates, effectiveness, and pressure drop. The 20-row heat pipes exhibited stable efficiency and acceptable pressure drop. They used 70 heat pipes in staggered arrangements of four and three tubes.

Nogueira[2] uses a theoretical model to calculate the thermal performance of heat exchangers with individually finned heat pipes. The model is localized and applied individually to the evaporator, condenser, and heat exchanger regions. The quantities used for performance analysis were the number of fins per heat pipe, the number of heat pipes, the inlet temperatures, and the flow rates of hot and cold fluids. Freon 404A refrigerant was used as a working fluid for cooling the evaporator and energy recovery in the condenser. A comparison was made with global experimental data on the heat exchanger under analysis. It obtained air velocity, Nusselt number, heat transfer rate, thermal effectiveness, and air outlet temperature results. It demonstrated that the localized theoretical approach is consistent and can be used as a comprehensive analysis tool for heat exchangers using heat pipes.

Fakheri[3] introduced the concept of thermal efficiency for heat exchangers, which is determined using a factor called "the fin analogy number". A dimensionless number makes it possible to characterize different configurations of heat exchangers in a single functional formula based on the efficiency of an insulated fin at the end and constant area. The physical parameters that characterize the dimensionless number in question, the global heat transfer coefficient, and the relationship between the thermal capacities of the means that exchange heat with each other make it possible to determine the thermal efficiency automatically and elegantly. The developed method brought a theoretical alternative to the traditional Logarithmic Mean Temperature Difference (LMTD) and Number of Thermal Units (NTU) methods, with the advantage of not requiring additional empirical parameters. Based on the second law of thermodynamics, the analytical process has undoubtedly solved many practical problems.

Nogueira[4] uses the concept of thermal efficiency to determine the thermal performance of shell and tube heat exchangers with external fins. The problem involves cooling machine oil using non-spherical cylindrical nanoparticles of Boehmite Alumina. The main quantities used in the analysis are the thermal effectiveness, the thermal and viscous irreversibilities, and the thermodynamic Bejan number. It was determined that increasing the number of finned tubes from two to six tubes is cost-effective at the expense of the high viscous dissipation caused by the oil in the annular region. The introduction of nanoparticles shows a slight decrease in the Bejan number despite significantly improving thermal performance.

Nogueira[5] applies the second law of thermodynamics to obtain outlet temperatures of the fluids in a shell and tube heat exchanger. It uses the concepts of thermal efficiency, thermal effectiveness, and thermal irreversibility to get relevant results. Water flows in the shell, and a mixture of water and ethylene

glycol associated with nanoparticles flows in the tubes. Results for Reynolds number and heat transfer rate are used to justify the output data, demonstrating that the flow regime significantly affects the thermal performance of the heat exchanger.

Putra et al.[6] conducted an experimental procedure to analyze the thermal performance of heat pipes in heat recovery to reduce electricity consumption. The heat exchanger consists of several tubular heat pipes staggered in up to six rows. The fins were attached individually to each heat pipe. The experiments showed a strong influence of the air inlet temperature in the evaporator and the air inlet velocity.

Höhne[7] simulates through computational fluid dynamics (CFD) the heat and mass transfer processes in a heat pipe to analyze thermal performance and save energy. It uses a homogeneous multiphase model to simulate the heat pipe's evaporation, condensation, and phase change processes. He claims that there is reasonable agreement between the computational implementation and experimental results from the literature. He is confident that using advanced computational models will become analysis tools for heat exchangers using heat pipes.

Jouhara et al.[8] conducted a theoretical-experimental investigation of heat exchangers with multipass heat pipes. The system consists of copper heat pipes in a staggered configuration to transfer energy from a hot gas to water in the condenser. The experiment was carried out by changing the number of passages in the evaporator through several deflectors for a single section of the condenser. They report that changing the number of passes from one to 5 allows for a 25% improvement in the efficiency of the heat exchanger. Two theoretical models were implemented, LMTD and ε-NTU, to determine the heat exchanger outlet temperatures. The theoretical-experimental validation demonstrated that the LMTD model predicted the performance of the heat exchanger with a +15.5% error, while the maximum error obtained through the ε-NTU model was 19%.

Barrak[9] states that energy consumption has increased mainly in developing countries, and energy waste will also increase. He argues that air conditioning units are the primary energy consumers and that energy recovery could be feasible if energy recovery units are attached to air conditioning units. In this sense, he says, it is vital that researchers focus on energy recovery devices and that heat pipes are promising devices for accomplishing this task.

Jouhara et al.[10] recognize heat pipes as passive devices with no moving parts, more efficient for heat exchange between two fluids because of their high thermal conductivity. Due to their thermal superconductivity, they realize that adding heat pipes makes them ideal for industrial applications requiring a high heat transfer rate. They state that the applications of heat pipes range from low-temperature cryogenic applications to systems that work at very high temperatures. They point out that implementing heat pipes as waste heat recovery can reduce the cost of the process, with lower energy consumption, in several industrial sectors.

Abd El-Baky and Mohamed[11] claim that heat pipes are used for energy recovery in air conditioning systems. In these cases, heat pipes, such as in hospital operating rooms, are intended to recover sensible heat when the inlet and return air must not be mixed. They report using a fresh and return air current system connected to a heat pipe heat exchanger in an energy recovery system. Estimate the optimal effectiveness of the heat pipe heat exchanger and compare it with experimental data. They claim that the results show a 48% increase in efficiency and heat transfer to the evaporator when the fresh air temperature is raised to a convenient level. Furthermore, they claim that the enthalpy ratio increases to about 85% with the fresh air inlet temperature increase. They clarify that using heat pipes allows for transporting much heat over a considerable distance without additional energy input to the system.

Sukarno et al.[12] report that specific requirements related to thermal comfort in hospital operating rooms require the development of efficient systems for air conditioning and energy recovery in the form of heat, and that one method capable of accomplishing this task is the use of heat pipe heat exchangers. They describe experiments with heat pipe heat exchangers having three, six, and nine rows arranged in a staggered configuration, with four heat pipes in each row. They conduct theoretical analysis based on the ε-NTU model to predict the system's thermal performance under study. They determine a maximum efficiency of 62.6% in a system with nine rows of heat pipes. They conclude that the ε-NTU method can analyze energy recovery systems that apply heat pipes.

Abedalh et al.[13] test a heat pipe heat exchanger in an air conditioning system to reduce energy consumption. The tested heat exchanger consists of 40 copper heat pipes arranged in four rows. They performed several experiments and determined the effectiveness and rate of heat recovery at different air inlet velocities. The maximum level obtained for effectiveness was 64.6%, and the highest value of heat recovered was 923.4 watts.

Amini et al.[14] investigate the industrial heat storage process to reduce energy consumption. They use phase change material (PCM) for latent heat storage. For the use of PCMs, which have low conductivity, they used finned heat pipes loaded with water as working fluid incorporated in the PCM volume. The evaporation section of the heat pipe is heated through the condensation of a steam flow, which heats the tubes and the PCM tank, which has a melting temperature of 89 ℃ and a crystallization point of 77 ℃. The heat absorbed in the evaporator is discharged through the heat pipes to the PCMs in the condenser. They conclude that the experiments carried out do not correspond to optimized conditions, requiring further investigations to determine how the heat pipes should be incorporated into the idealized heat exchanger to improve the phase change rate of the PCM.

Hakim et al.[15] experimented with a finned U-shaped heat pipe heat exchanger (HPHE) in a vertical configuration to reduce building energy consumption. They present results for the effectiveness and dehumidification capacity of the U-shaped HPHE coupled to the heating, ventilation, and air conditioning (HVAC) system. Demonstrate that two-row U-shaped HPHE increases the 39.9% coefficient of performance over HVAC without HPHE and can reduce 21.6% relative humidity, which results in energy savings for pre-cooling and heating. They conclude that the U-shaped finned heat pipe is a solution for upgrading an HVAC system.

2. Methodology

The system under analysis was experimentally evaluated and published by Górecki et al.[1]. The schematic diagram of the equipment can be found in **Figure 1** of the work mentioned above. It consists of heat pipes with individual fins (IFHPHE).

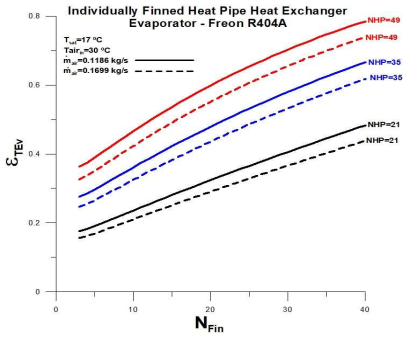

Figure 1. Thermal effectiveness versus fin number in the evaporator section.

The saturation temperature of the working fluid (R404A) in the heat pipe is represented by Equation (1).

$$T_{sat} = 17.0\ ℃\ fixed\ by\ definition \tag{1}$$

The saturation pressure of the working fluid (R404A) can be obtained through Equation (2):

$$P_{sat} = 614.1316315 + 17.18802462T_{sat} + 0.3276728108T_{sat}^2 \tag{2}$$

Equations (3)–(21) represent the properties of the working fluid (R404A) as a function of the saturation temperature. All properties were taken from literature tables valid for the element under analysis, and the numerical determination through polynomials was obtained through graphic software.

$$\rho_l = 1148.516119 - 2.934024895T_{sat} - 0.0425519003T_{sat}^2 \tag{3}$$

$$\rho_v = 29.62609253 + 1.088373933T_{sat} + 0.002241182059T_{sat}^2 + 0.0003618637607T_{sat}^3 \tag{4}$$

$$h_l = 200.2774524 + 1.356658428T_{sat} + 0.00586628846T_{sat}^2 \tag{5}$$

$$h_v = 368.3562439 + 0.5331782112T_{sat} - 0.0005307756065T_{sat}^2 - 6.0092036610^{-5}T_{sat}^3 \tag{6}$$

$$h_{lv} = h_v - h_l \tag{7}$$

Table 1 presents the properties of the working fluid (R404A).

Table 1. Properties of the working fluid (R404A) at saturation temperature.

T_{sat} ℃	$\rho_l \frac{kg}{m^3}$	$\rho_v \frac{kg}{m^3}$	$h_l\ -J/kg$	$h_v\ -J/kg$	$h_{lv}\ -J/kg$
17.0	1086.34	50.55	225.04	376.97	151.94

$$P_{sat} = 1001.02\ \text{Pa} \tag{8}$$

$$k_{R404l} = 0.0863\ \frac{W}{mK} \tag{9}$$

$$k_{R404v} = 0.01346 \tag{10}$$

$$Cp_{R404l} = 1530 \tag{11}$$

$$Cp_{R404v} = 870 \tag{12}$$

$$\mu_{R404l} = 1.2810^{-4} \tag{13}$$

$$\mu_{R404v} = 1.2210^{-5} \tag{14}$$

$$\nu_{R404l} = \frac{\mu_{R404l}}{\rho_{R404l}} \tag{15}$$

$$\nu_{R404v} = \frac{\mu_{R404v}}{\rho_{R404v}} \tag{16}$$

$$\rho_{R404l} = 1086.34 \tag{17}$$

$$\alpha_{R404l} = \frac{k_{R404l}}{\rho_{404l}Cp_{404l}} \tag{18}$$

$$\alpha_{R404v} = \frac{k_{R404v}}{\rho_{404v}Cp_{404v}} \tag{19}$$

$$Pr_{R404l} = \frac{\nu_{R404l}}{\alpha_{R404l}} \tag{20}$$

$$Pr_{R404v} = \frac{\nu_{R404v}}{\alpha_{R404v}} \tag{21}$$

The number of rows of Heat Pipes (HP) is defined by Equation (22).

$$N_{rows} = 3\ default;\ 3 \le N_{rows} \le 21 \tag{22}$$

Equation (23) represents the total number of heat pipes in the heat exchanger, and the number of fins $\boldsymbol{N_{Fin}}$ considered in the evaporator or condenser is defined by Equation (24). Equation (25) represents the volume flow rate of the air.

$$NHP = \frac{N_{rows}}{3}(3+4);\ 7 \le NHP \le 49 \tag{23}$$

$$N_{Fin} = 30default;\ 0 \le N_{Fin} \le 70 \tag{24}$$

$$\dot{V}_{air} = \frac{370.0}{3600}\frac{m^3}{s}default;\ \frac{370.0}{3600} \le \dot{V}_{air} \le \frac{550.0}{3600} \tag{25}$$

The properties of the air, dependent on the inlet temperature $\boldsymbol{Tair_{in}}$, can be obtained by the following Equations (26)–(29). All properties were taken from literature tables valid for the element under analysis, and the numerical determination through polynomials was obtained through graphic software.

Equation (26) is represented by thermal conductivity, and the dynamic, absolute viscosity of air characterizes Equation (27). The specific heat of air represents Equation (28). The density of the air is represented by Equation (29).

$$k_{air} = 6.91744186\ 10^{-5}Tair_{in} + 0.02462173663 \tag{26}$$

$$\mu_{air} = 1.95483621\ 10^{-5} + 2.735058039\ 10^{-9}Tair_{in} + 2.309587479\ 10^{-10} Tair_{in}^2 - 4.505882353\ 10^{-13}Tair_{in}^3 \tag{27}$$

$$Cp_{air} = 1003.728948 + 0.06727399886 * Tair_{in} + 3.565918367\ 10^{-6} Tair_{in}^2 + 8.222222222\ 10^{-7}Tair_{in}^3 \tag{28}$$

$$\rho_{air} = 1.219135515 - 0.002152770329Tair_{in} - 3.64047479\ 10^{-7}Tair_{in}^2 + 1.705882353\ 10^{-9}Tair_{in}^3 \tag{29}$$

Table 2 presents air properties at the reference temperature.

Table 2. Air properties at the reference temperature.

$\boldsymbol{Tair_{in}}$ ℃	$\boldsymbol{k_{air}} - \frac{\boldsymbol{W}}{\boldsymbol{mK}}$	$\boldsymbol{\mu_{air}} - \frac{\boldsymbol{kg}}{\boldsymbol{ms}}$	$\boldsymbol{\rho_{air}} - \frac{\boldsymbol{kg}}{\boldsymbol{m^3}}$	$\boldsymbol{Cp_{air}} - \frac{\boldsymbol{J}}{\boldsymbol{kgK}}$
30.0 ℃	2.67×10^{-2}	1.98×10^{-5}	1.15	1005.77

$$\nu_{air} = \frac{\mu_{air}}{\rho_{air}} \tag{30}$$

$$\alpha_{air} = \frac{k_{air}}{\rho_{air}Cp_{air}} \tag{31}$$

Equation (32) represents the Prandtl number associated with the air.

$$Pr_{air} = \frac{\nu_{air}}{\alpha_{air}} \tag{32}$$

The surface tension for water, represented by $\boldsymbol{\sigma_{Water}}$, is given by Equation (33)[10].

$$\sigma_{Water} = 0.07275\big(1 - 0.002(K - 291)\big) \tag{33}$$

where $\boldsymbol{K}$ is saturation temperature in Kelvin.

The assumed constant for the surface-fluid combination represents Equation (34)[16].

$$C_{sf} = 0.006 \tag{34}$$

The mass flow rate of air at the inlet of the heat exchanger $\dot{m}_{air}$ is defined by Equation (35).

$$\dot{m}_{air} = \rho_{air}\dot{V}_{air} \tag{35}$$

The localized analytical approach is subdivided into the evaporator, the condenser, and the global Finned Heat Pipe Heat Exchanger (FHPHE).

2.1. Equations for the evaporator section of the heat exchanger

In the evaporator region, during the cooling of the heated fresh air, the inlet temperature of the heated fresh air varies between 20 °C and 50 °C. The inlet volume flow rate of fresh heated air in the evaporator region varies between 0.1078 m^3/s and 0.1528 m^3/s.

The formulation to simulate the heat exchange process in the evaporator is established through Equations (36)–(87).

The fresh air inlet temperature in the evaporator region, defined by Equation (36), is represented by $\boldsymbol{TEv_{in}}$.

$$TEv_{in} = 30.0\ ℃\ default;\quad 20.0\ ℃ \le TE_{in} \le 50.0\ ℃ \tag{36}$$

The estimated heat transfer coefficient for the boiling process, initially presented by Rohsenow[16] and related by Jouhara et al.[10], is given by $\boldsymbol{h_{boil}}$.

$$h_{boil} = \mu_l h_{lv}\left(\frac{g(\rho_l - \rho_v)}{\sigma_{water}}\right)^{1/2}\left(\frac{Cp_l}{C_{sf}h_{lv}Pr_l}\right)^3 \Delta T_{sat}^2 \tag{37}$$

$$\Delta T_{Evsat} = TEv_{in} - T_{sat} \tag{38}$$

The outside and inside diameters of the heat pipe are represented by $\boldsymbol{D_{ext}}$ and $\boldsymbol{D_{int}}$ are given by Equation (39), Equation (40)[1].

$$D_{ext} = 22.0\ 10^{-3}\ m \tag{39}$$

$$D_{\text{int}} = 20.010^{-3}\ m \tag{40}$$

The thermal conductivity of the heat pipe material (Copper), represented by Equation (41), is given by $\boldsymbol{k_W}$.

$$k_W = 235.0 \tag{41}$$

$\boldsymbol{LEv}$, illustrated by Equation (42), is the length of the heat pipe evaporation section and $\boldsymbol{WHE}$, represented by Equation (43), is the shell's width.

$$LEv = 250.010^{-3} \tag{42}$$

$$WHE = 200.0\ 10^{-3} \tag{43}$$

$$t_{Fin} = 0.810^{-3} \tag{44}$$

The thermal conductivity of the fin material (Aluminum) is given by $\boldsymbol{k_{Fin}}$.

$$k_{Fin} = 401.0 \tag{45}$$

The effective heat exchange length associated with the heat pipes in the evaporator is obtained by $\boldsymbol{LEv_{effec}}$. The thickness of a fin represented is given by $\boldsymbol{t_{Fin}}$. The space between fins, defined through Equation (46), is provided by $\boldsymbol{Sp_{Fin}}$.

$$Sp_{Fin} = 2.5\ 10^{-3}\ by\ definition \tag{46}$$

$$LEv_{effec} = LEv - NFin(t_{Fin} + Sp_{Fin}) \tag{47}$$

The hydraulic diameter of the heat exchanger in the evaporator region is given by $\boldsymbol{Dh_{Ev}}$. The Reynolds number associated with air, represented by Equation (49), is provided by $\boldsymbol{Re_{air}}$.

$$Dh_{EV} = \frac{4WHELEv_{effec}}{2(WHE + LEv_{effec})} \tag{48}$$

$$Re_{air} = \frac{4\dot{m}_{air}}{\pi Dh_{Ev}\mu_{air}} \tag{49}$$

Equation (50) represents the effective area occupied by the air in the evaporator.

$$A\,sec_{air} = \frac{\dot{m}_{air} Dh_{Ev}}{Re_{air}\,\mu_{air}} \tag{50}$$

The air velocity in the evaporator is represented by $\boldsymbol{V_{air}}$.

$$V_{air} = \frac{\dot{m}_{air}}{A\,sec_{air}\,\rho_{air}} \tag{51}$$

$$Dext_{Fin} = 50.010^{-3} \tag{52}$$

$$D\,int_{Fin} = D_{ext} \tag{53}$$

The effective heat transfer area in the evaporator Atr_{HP}, associated with heat pipes, is established by Equation (55). The effective heat transfer area associated with the fin system, Atr_{Fin}, and the total heat transfer area, A_{Total}, are represented by Equations (54), Equations (56).

$$Atr_{Fin} = NFinNHP\frac{\pi}{4}(Dext_{Fin}^2 - D\,int_{Fin}^2) \tag{54}$$

$$Atr_{HP} = NHP\pi D_{ext}(LEv - NFinSp_{Fin}) \tag{55}$$

$$A_{Total} = Atr_{Fin} + Atr_{HP} \tag{56}$$

$$Vair_{\max} = \frac{\dot{V}_{air}}{A\sec_{air}} \tag{57}$$

$$dr = 24.010^{-3}\ assumed \tag{58}$$

$$Re_{dr} = \frac{Vair_{max}}{v_{air}} \tag{59}$$

The Nusselt number for the air, as reported by Górecki et al.[1] is represented by $\boldsymbol{Nu_{air}}$. The convection heat transfer coefficient associated with air in the Evaporator is given by $\boldsymbol{h_{air}}$.

$$Nu_{air} = 0.1387\,\mathrm{Re}_{dr}^{0.718}\,\mathrm{Pr}_{air}^{(1/3)}\left(\frac{Sp_{Fin}}{Dext_{Fin} - D\,\mathrm{int}_{Fin}}\right)^{0.296} \tag{60}$$

$$h_{air} = \frac{Nu_{air}k_{air}}{dr} \tag{61}$$

$$mL_{Fin} = \sqrt{\frac{2h_{sair}}{k_{Fin}t_{Fin}}}\,t_{Fin} \tag{62}$$

The fin efficiency for the evaporator section is defined by $\boldsymbol{\eta_{Fin}}$[11].

$$\eta_{Fin} = \frac{\mathrm{Tanh}(mL_{Fin})}{mL_{Fin}} \tag{63}$$

$$\beta = \frac{Atr_{Fin}}{A_{Total}} \tag{64}$$

The efficiency associated with the set of fins in the evaporator, weighted by the area of heat exchange of the fins, is represented through $\boldsymbol{\eta'_{Fin}}$.

$$\eta'_{Fin} = \beta\eta_{Fin} + (1 - \beta) \tag{65}$$

The global heat transfer coefficient associated with air in the evaporator, Uo_{Ev}, is given by Equation (66).

$$Uo_{Ev} = \frac{1}{\frac{1}{h_{boil}} + \frac{D_{ext} - D_{int}}{kW} + \frac{1}{\eta_{Fin}^{'} h_{air}}} \tag{66}$$

The heat capacity of the air in the evaporator is given by C_{Air}.

$$C_{Air} = \dot{m}_{air} Cp_{air} \tag{67}$$

$$C_{Ev} = C_{air} \tag{68}$$

The number of thermal units associated with air in the evaporator, NTU_{Ev}, is given by Equation (69).

$$NTU_{Ev} = \frac{Uo_{Ev} A_{Total}}{CEv} \tag{69}$$

The dimensionless number, called "fin analogy", is represented $\boldsymbol{Fa}$as defined by Fakheri[3] and reported by Nogueira[5].

$$Fa = \frac{NTU\sqrt{1 + C^{*2}}}{2} \; for \; cross - flow \tag{70}$$

The thermal efficiency associated with the heat exchanger is $\boldsymbol{\eta_T}$[11].

$$\eta_T = \frac{tanh(Fa)}{Fa} \tag{71}$$

The thermal effectiveness related to the heat exchanger is $\boldsymbol{\varepsilon_T}$[11].

$$\varepsilon_T = \frac{1}{\frac{1}{\eta NTU} + \frac{1 + C^*}{2}} \tag{72}$$

The heat exchanger's thermal efficiency depends on two fundamental parameters: $\boldsymbol{NTU}$ e $\boldsymbol{C^*} = \frac{\boldsymbol{C_{min}}}{\boldsymbol{C_{max}}}$. For the physical conditions under analysis $\boldsymbol{C^*} = \boldsymbol{0.0}$. Then,

$$Fa_{Ev} = \frac{NTU_{Ev}}{2} \tag{73}$$

$$\eta_{TEv} = \frac{tanh(Fa_{Ev})}{Fa_{Ev}} \tag{74}$$

$$\varepsilon_{TEv} = \frac{1}{\frac{1}{\eta_{TEv} NTU_{Ev}} + \frac{1}{2}} \tag{75}$$

The heat transfer rate between the air and the heat pipe in the evaporating region is given by $\dot{\boldsymbol{Q}}_{\boldsymbol{Ev}}$.

$$\dot{Q}_{Ev} = \frac{C_{Ev} \Delta T_{Evsat}}{\frac{1}{\eta_{TEv} NTU_{Ev}} + \frac{1}{2}} \tag{76}$$

After passing through the evaporator, the outlet air temperature is represented through Equation (77).

$$TEv_{out} = TEv_{in} - \frac{\dot{Q}_{Ev}}{C_{Ev}} \tag{77}$$

$$X_t = Dext_{Fin} \tag{78}$$

$\boldsymbol{f_{Ev}}$, represented by Equation (79), is the friction factor associated with the flow rate in the evaporator. In this work, for the configuration under analysis and some fins equal to 30, the coefficient value was conveniently adjusted to 0.7465.

$$f_{Ev} = 0.7465\,\mathrm{Re}_{dr}^{(-0.316)}\left(\frac{X_t}{dr}\right)^{(-0.927)} \tag{79}$$

Δp_{Ev} , represented by Equation (80), is the pressure drop in the evaporator.

$$\Delta p_{Ev} = 2 f_{Ev} N_{rows} \rho_{air} Vair_{max} \tag{80}$$

The thermal irreversibility in the evaporator is represented by Equation (81).

$$\sigma_{TEv} = ln\left(\frac{TEv_{in}}{TEv_{out}}\right) \tag{81}$$

The entropy generation associated with the thermal field in the evaporator is represented by Equation (82).

$$\dot{S}_{genTEv} = \sigma_{TEv} C_{Ev} \tag{82}$$

$\boldsymbol{P_{2Ev}}$ is the outlet pressure in the evaporator.

$$P_{2Ev} = P_{atm} + \Delta p_{Ev} \tag{83}$$

$$Rh_{Ev} = \frac{TEv_{in} - TEv_{out}}{TEv_{in} - T_{sat}} \tag{84}$$

$\boldsymbol{\sigma_{fEv}}$ is the viscous irreversibility in the evaporator.

$$\sigma_{fEv} = Rh_{Ev} \ln\left(\frac{P_{atm}}{P_{2Ev}}\right) \tag{85}$$

The entropy generation associated with the flow field in the evaporator is represented by Equation (86).

$$\dot{S}_{genfEv} = \sigma_{fEv} C_{Ev} \tag{86}$$

The thermodynamic Bejan number in the evaporator is represented by Equation (87).

$$Be_{Ev} = \frac{\dot{S}_{genTEv}}{\dot{S}_{genTEv} + \dot{S}_{genfEv}} \tag{87}$$

2.2. Equations for the condenser section of the heat exchanger

The air conditioning is sucked through the exhaust pipes and passes through the heat pipe condenser region. The saturation temperature of the working fluid is higher than the temperature of the air conditioning, which varies between 0 ℃ and 15 ℃. The inlet volume flow rate of the air conditioning in the condenser region varies between 0.1028 m^3/s and 0.1472 m^3/s[1].

The formulation used to simulate the heat exchange process in the condenser is established through Equations (88)–(113).

The air temperature at the condenser inlet, $\boldsymbol{TCd_{in}}$, is represented by Equation (88).

$$TCd_{in} = 0.0\ ℃\ ;\ 0.0\ ℃ \le TCd_{in} \le 15.0\ ℃ \tag{88}$$

Equation (89) represents the temperature difference between the condenser's air and the working fluid.

$$\Delta T_{Cdsat} = T_{sat} - TCd_{in} \tag{89}$$

The condenser section's length is represented through Equation (90).

$$LCd = LEv \tag{90}$$

Equation (91) represents the effective length of the condenser for the heat exchange.

$$LCd_{effec} = LCd - N_{Fin}(t_{Fin} + Sp_{Fin}) \tag{91}$$

The hydraulic diameter in the region of the capacitor, $\boldsymbol{Dh_{Cd}}$, is represented by Equation (92).

$$Dh_{Cd} = \frac{4WHELCd_{effec}}{2(WHE + LCd_{effec})} \tag{92}$$

The Reynolds number of air in the condenser region, $\boldsymbol{Re_{air}}$, is represented through Equation (93).

$$Re_{air} = \frac{4\dot{m}_{air}}{\pi Dh_{Cd}\mu_{air}} \tag{93}$$

The airflow area in the condenser, $A\sec_{air}$, is given by Equation (94).

$$A\,sec_{air} = \frac{\dot{m}_{air}Dh_{Cd}}{Re_{air}\,\mu_{air}} \tag{94}$$

The condensation transfer coefficient in the heat pipe is provided by $\boldsymbol{h_{Cond}}$, as reported by Nogueira[5].

$$h_{Cond} = 0.943[\frac{[\rho_l(\rho_l - \rho_v)h_{lv}gk_W^3]}{(\mu_W LCd\Delta T_{sat})}]^{1/4} \tag{95}$$

$$Uo_{Cd} = \frac{1}{\frac{1}{h_{Cond}} + \frac{D_{ext} - D_{int}}{kW} + \frac{1}{\eta_{Fin}^{'}h_{air}}} \tag{96}$$

Equation (96) represents the global heat transfer coefficient.

$$C_{Air} = \dot{m}_{air}Cp_{air} \tag{97}$$

The air's heat capacity in the condenser's region is characterized by $\boldsymbol{C_{Cd}}$.

$$C_{Cd} = C_{air} \tag{98}$$

Equation (99) represents the number of thermal units associated with the heat pipes in the condenser region.

$$NTU_{Cd} = \frac{Uo_{Cd}A_{Total}}{C_{Cd}} \tag{99}$$

The dimensionless parameter called "fin analogy" in the condenser region is represented $\boldsymbol{Fa_{Cd}}$.

$$Fa_{Cd} = \frac{NTU_{Cd}}{2} \tag{100}$$

Equation (101) represents the thermal efficiency associated with the condenser.

$$\eta_{TCd} = \frac{tanh(Fa_{Cd})}{Fa_{Cd}} \tag{101}$$

Equation (102) represents the thermal effectiveness related to the condenser.

$$\varepsilon_{TCd} = \frac{1}{\frac{1}{\eta_{TCd}NTU_{Cd}} + \frac{1}{2}} \tag{102}$$

The heat transfer rate between the air and the heat pipe in the condenser region is characterized by Equation (103).

$$\dot{Q}_{Cd} = \frac{C_{Cd}\Delta T_{Cdsat}}{\frac{1}{\eta_{TCd}NTU_{Cd}} + \frac{1}{2}} \tag{103}$$

The air outlet temperature in the condenser is represented through $\boldsymbol{TCd_{out}}$.

$$TCd_{out} = \frac{\dot{Q}_{Cd}}{C_{Cd}} + TCd_{in} \tag{104}$$

$\boldsymbol{f_{Cd}}$, illustrated by Equation (105), is the friction factor associated with the flow in the condenser.

$$f_{Cd} = 0.7465\,\mathrm{Re}_{dr}^{(-0.316)}\left(\frac{X_t}{dr}\right)^{(-0.927)} \tag{105}$$

Δp_{Cd}, represented by Equation (106), is the pressure drop in the condenser.

$$\Delta p_{Cd} = 2 f_{Cd} N_{rows} \rho_{air} Vair_{max} \tag{106}$$

The thermal irreversibility in the condenser is represented by Equation (107).

$$\sigma_{TCd} = ln\left(\frac{TCd_{in}}{TCd_{out}}\right) \tag{107}$$

The entropy generation associated with the thermal field in the condenser is represented by Equation (108).

$$\dot{S}_{genTCd} = \sigma_{TCd} C_{Cd} \tag{108}$$

$\boldsymbol{P_{2Cd}}$ is the outlet pressure in the condenser.

$$P_{2Cd} = P_{atm} + \Delta p_{Cd} \tag{109}$$

$$Rh_{Cd} = \frac{TCd_{in} - TCd_{out}}{TCd_{in} - T_{sat}} \tag{110}$$

$\boldsymbol{\sigma_{fCd}}$ is the viscous irreversibility in the condenser.

$$\sigma_{fCd} = Rh_{Cd} \ln\left(\frac{P_{atm}}{P_{2Cd}}\right) \tag{111}$$

The entropy generation associated with the flow field in the condenser is represented by Equation (112).

$$\dot{S}_{genfCd} = \sigma_{fCd} C_{Cd} \tag{112}$$

The thermodynamic Bejan number in the condenser is represented by Equation (113).

$$Be_{Cd} = \frac{\dot{S}_{genTCd}}{\dot{S}_{genTCd} + \dot{S}_{genfCd}} \tag{113}$$

2.3. Equations for individually finned heat pipe crow-flow heat exchanger (IFHPHE)

The cooling and energy recovery set to form a heat exchanger, with a fresh air inlet with a temperature above 17 °C and a cooled air outlet below 17 °C. The total heat transfer rate in the air conditioning process is equal to the sum of the heat transfer rates in the evaporator and the condenser $\boldsymbol{\dot{Q}_{Cd}}$, according to Equation (114). Equation (115) represents the maximum transfer rate, $\boldsymbol{\dot{Q}_{Max}}$, in the heat exchanger, which $\boldsymbol{C_{min}}$ is the smallest of the thermal capacities of the air involved in the process. Equation (116) represents the heat exchanger's effectiveness in air conditioning.

$$\dot{Q}_{IFHPHE} = \dot{Q}_{Ev} + \dot{Q}_{Cd} \tag{114}$$

$$\dot{Q}_{Max} = C_{\min}(TEv_{in} - TCd_{out}) \tag{115}$$

$$\varepsilon_{IFHPHE} = \frac{\dot{Q}_{IFHPHE}}{\dot{Q}_{Max}} \tag{116}$$

$$\Delta p_{IFHPHE} = \Delta p_{Ev} + \Delta p_{Cd} \tag{117}$$

$$\sigma_{THPHE} = \sigma_{TEv} + \sigma_{TCd} \tag{118}$$

$$\sigma_{fHPHE} = \sigma_{fEv} + \sigma_{fcd} \tag{119}$$

$\boldsymbol{Be_{HPHE}}$ is the thermodynamic Bejan number associated with the heat exchanger.

$$Be_{HPHE} = \frac{\sigma_{THPHE}}{\sigma_{THPHE} + \sigma_{fHPHE}} \quad (120)$$

3. Results and discussion

The thermal effectiveness in the evaporator section is analyzed for two air mass flow rates, within a borderline range for the air conditioning system $\dot{m}_{air} = \mathbf{0.1699}\ kg/s$, in **Figure 1** The variables used in the analysis are the number of fins per heat pipe and the number of heat pipes. Effectiveness decreases with increasing airflow and increases with the number of fins and heat pipes. For example, for multiple fins equal to 40 and heat pipes equal to 49, the thermal efficiency reaches a value close to 80%. When the number of heat pipes equals 21, the thermal effectiveness reaches 40% for the smallest flow rate. The thermal effectiveness is relatively high in all analyzed situations, and it is what is expected for a well-dimensioned heat exchanger.

The heat transfer rate in the evaporator, **Figure 2**, has the same trend as the effectiveness in qualitative terms. However, the maximum value for the heat transfer rate occurs for the highest mass flow rate of air due to the highest heat capacity. The highest observed heat transfer rate is for $\boldsymbol{NHP = 49}$ and $\boldsymbol{N_{Fin} = 40}$, as expected.

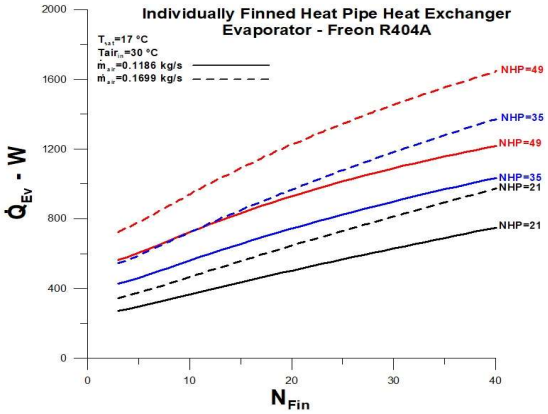

Figure 2. Heat transfer rate versus fin number in the evaporator section.

The thermal irreversibility of the evaporator is represented in **Figure 3** and shows a growth trend similar to that of thermal effectiveness in qualitative terms. The most significant thermal irreversibility is observed for $\boldsymbol{NHP = 49}$ and $\boldsymbol{N_{Fin} = 40}$, with a value close to 0.45 for lower airflow. A high value for thermal effectiveness is expected for heat exchangers.

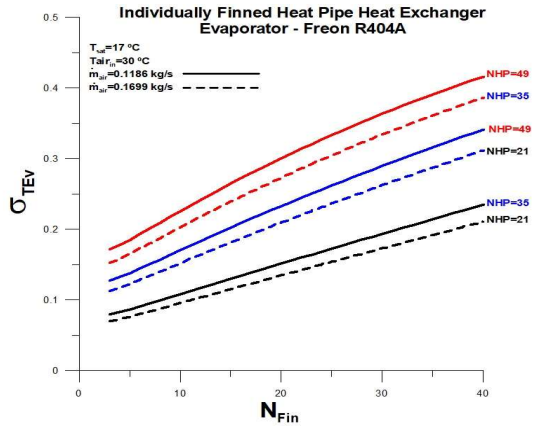

Figure 3. Thermal irreversibility versus fin number in the evaporator section.

The air outlet temperature in the evaporator region is represented in **Figure 4** for an air inlet temperature equal to 30 °C and a Freon saturation temperature equal to 17 °C. The temperature decreases with an increasing number of heat pipes and the number of fins. The lowest air outlet temperature is obtained for the most downward airflow over-analysis. The lowest value corresponds to approximately 19 °C, for $NHP = 49$, $N_{Fin} = 40$ e $\dot{m}_{air} = 0.1186\ kg/s$.

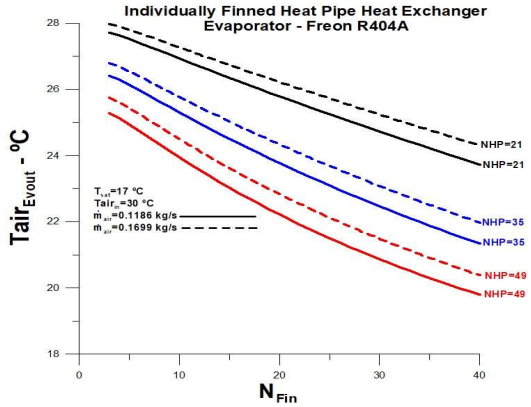

Figure 4. Air outlet temperature versus fin number in the evaporation section.

Figure 5 shows the pressure drop in the evaporator region as a function of the number of fins per heat pipe, the number of heat pipes, and the airflow. As expected, the increase in air flow significantly increases the pressure drop in the evaporator. The highest value obtained for the pressure drop in the evaporator corresponds to approximately 120 Pa, for $NHP = 49$, $N_{Fin} = 40$ e $\dot{m}_{air} = 0.1699\ kg/s$.

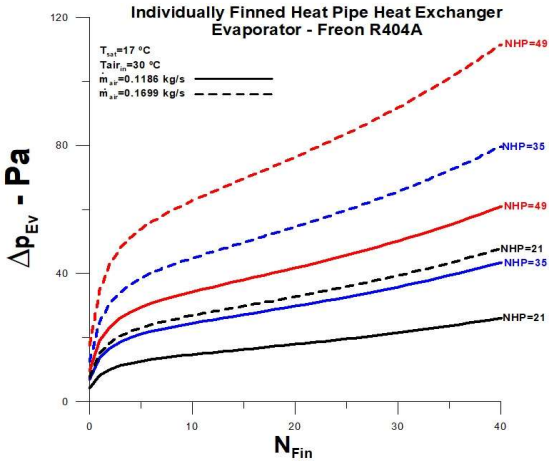

Figure 5. Pressure drops versus fin number in the evaporation section.

The viscous irreversibility in the evaporator shows a growth trend similar to the pressure drop, as seen in **Figure 6**. The highest value obtained for the thermal irreversibility in the evaporator corresponds to approximately 60%, for $NHP = 49$,$N_{Fin} = 40$ e $\dot{m}_{air} = 0.1699\ kg/s$. High viscous irreversibility is detrimental in terms of cost for a heat exchanger.

The number of fins per heat pipe and the number of heat pipes in the evaporator region significantly affect the value of the Bejan number, **Figure 7**. The smallest value for the Bejan number is observed for $NHP = 49$, $N_{Fin} = 40$ e $\dot{m}_{air} = 0.1699\ kg/s$**,** numerically, approximately equal to 0.4. The highest value observed for the Bejan number corresponds roughly to 0.9 for heat pipes without fins and lower

airflow due to lower viscous irreversibility. The lower number of heat pipes, $NHP = 21$, and the higher number of fins enable a high cost-benefit ratio above 0.7.

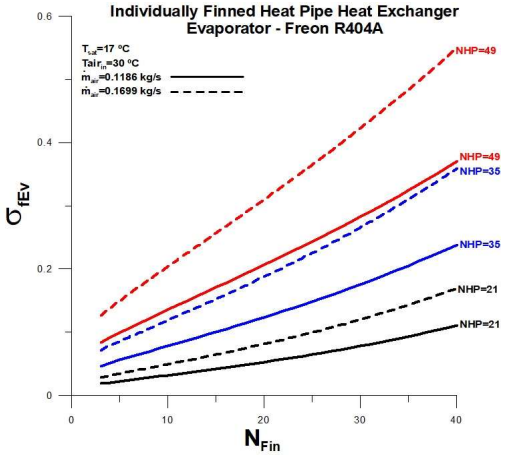

Figure 6. Viscous irreversibility versus fin number in the evaporation section.

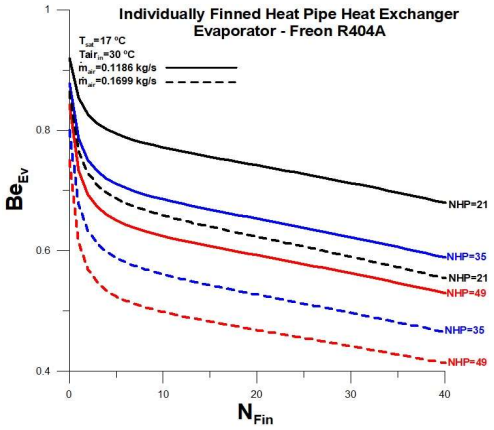

Figure 7. Bejan number versus fin number in the evaporation section.

The thermal effectiveness in the condenser section is analyzed for two air mass flow rates, within a borderline range for the air conditioning system, that is, $\dot{m}_{air} = 0.1186\ kg/s$ e $\dot{m}_{air} = 0.1699\ kg/s$, in **Figure 8**. The variables used in the analysis are the number of fins per heat pipe and the number of heat pipes. Effectiveness decreases with increasing airflow and increases with the number of fins and heat pipes. For example, for some fins equal to 40 and heat pipes equal to 49, the effectiveness reaches a value close to 70%.

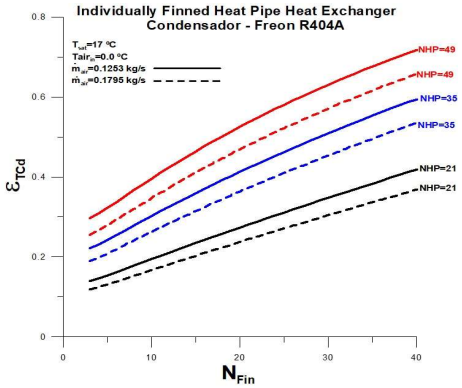

Figure 8. Thermal effectiveness versus fin number in the condenser section.

The heat transfer rate in the condenser, **Figure 9**, has the same trend as the effectiveness in qualitative terms. However, the maximum value for the heat transfer rate occurs for the highest mass flow rate of air due to the highest heat capacity—the highest observed heat transfer rate for $\boldsymbol{NHP = 49}$ e $\boldsymbol{N_{Fin} = 40}$.

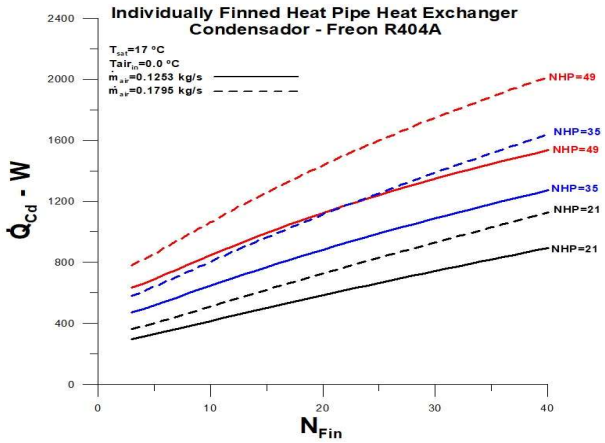

Figure 9. Heat transfer rate versus fin number in the condenser section.

The air outlet temperature in the condenser region is represented in **Figure 10** for an air inlet temperature equal to 0.0 °C and a Freon saturation temperature equal to 17 °C. The outlet temperature increases with an increasing number of heat pipes and the number of fins. The highest air outlet temperature is obtained for the lowest airflow over-analysis. The highest value corresponds to approximately 13 °C, for $\boldsymbol{NHP = 49}$, $N_{Fin} = 40$ e $\boldsymbol{\dot{m}_{air} = 0.1253\ kg/s}$.

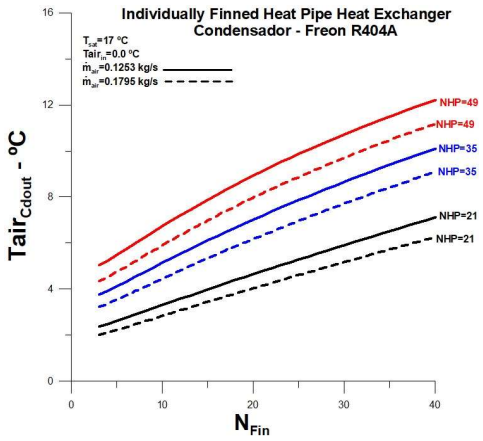

Figure 10. Air outlet temperature versus fin number in the condenser section.

Figure 11 shows the pressure drop in the condenser region as a function of the number of fins per heat pipe, the number of heat pipes, and the airflow. As expected, the increase in air flow significantly increases the pressure drop in the evaporator. The highest value obtained for the head loss in the evaporator corresponds to approximately 120 Pa, for $\boldsymbol{NHP = 49}$,$\boldsymbol{N_{Fin} = 40}$ e $\boldsymbol{\dot{m}_{air} = 0.1795\ kg/s}$.

The number of fins per heat pipe and the number of heat pipes in the condenser region significantly affect the value of the Bejan number, **Figure 12**. The lowest value for the Bejan number is observed for $\boldsymbol{NHP = 49}$ e $\boldsymbol{N_{Fin} = 40}$ and $\boldsymbol{\dot{m}_{air} = 0.1795\ kg/s}$, numerically, approximately equal to 0.4. The highest value observed for the Bejan number corresponds roughly to 0.95 for heat pipes without fins and lower airflow due to lower viscous irreversibility. There is less heat exchange without fins, but the relative weight between thermal irreversibility and total irreversibility is high.

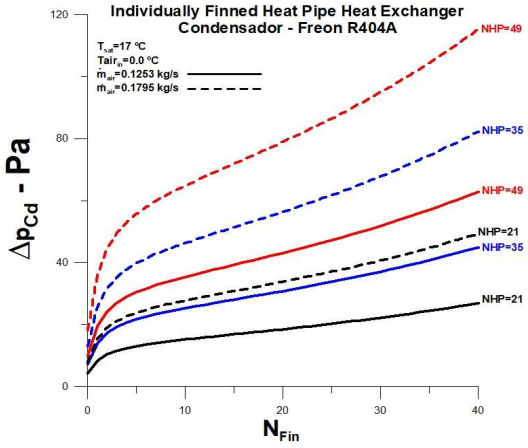

Figure 11. Pressure drops versus fin number in the condenser section.

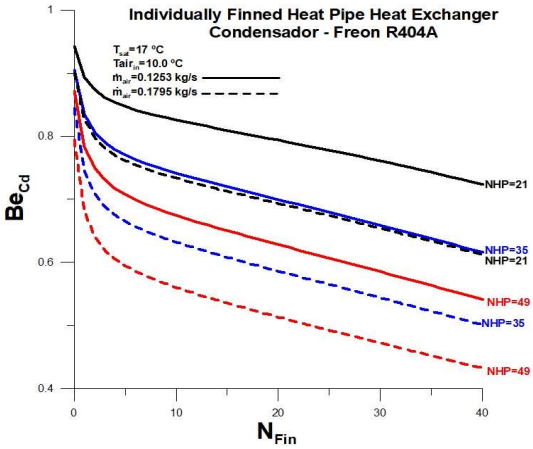

Figure 12. Bejan number versus fin number in the condenser section.

Figure 13 presents theoretical and experimental results for the heat transfer rate for the heat exchanger under analysis. The experimental data has shown that when compared with the theoretical results, demonstrate that the number of fins in the heat exchanger is between 10 and 40 fins and that the observed theoretical trend is compatible with the experiment since the total transfer rate of heat tends to grow with the number of rows and with the number of fins. The thermal effectiveness tends to be the maximum possible when the number of fins is equal to 40 and the number of heat pipes is equal to 49 since, in this case, the heat transfer rate coincides with the maximum value (**Figure 14**).

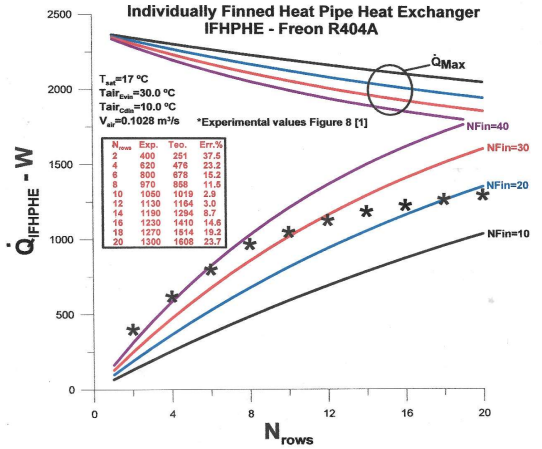

Figure 13. Heat transfer rate for the heat exchanger versus the number of rows.

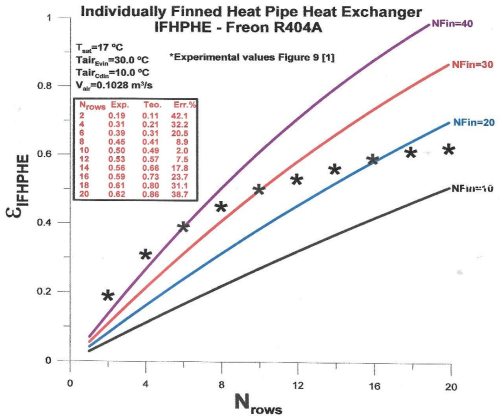

Figure 14. Effectiveness of the heat exchanger versus the number of rows.

When comparing the total theoretical pressure drop with experimental results, it is evident that the number of fins in the original heat exchanger is equal to 30 fins, as shown in **Figure 15**. However, the theoretical value results from the stipulated coefficient in the friction factor Equation (79), Equation (105), and once again, the theoretical results obtained are consistent with what is expected with the total pressure drop when increasing the number of fins from 10 to 40.

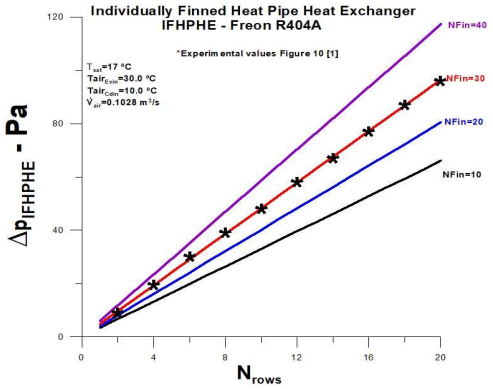

Figure 15. Total pressure drops versus the number of rows.

Figure 16 presents results for the thermodynamic Bejan number related to the heat exchanger. The highest cost-benefit ratio is associated with the lowest number of fins per heat pipe, equal to 10. However, fins equal to 10 correspond to the lowest heat transfer rate, as shown in **Figure 13**. There must be a compromise between the number of fins and the outlet temperature of the air. **Figure 10** shows a more significant number of fins and a greater number of heat pipes, allowing for a higher outlet temperature.

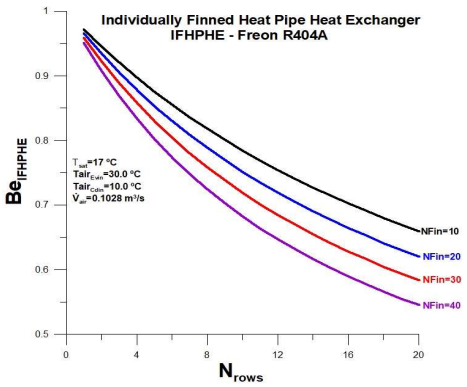

Figure 16. Bejan thermodynamic number for heat exchanger versus the number of rows.

It is evident that there must be a compromise with all the analyzed factors, and a satisfactory cost-benefit ratio, thermal irreversibility versus total irreversibility, must be sought. In this sense, it is concluded that fins between 10 and 20 for heat pipes equal to 49 provide a better cost-benefit ratio.

The results obtained individually and globally are adequate and consistent concerning the expected values for all the quantities analyzed. The global results for the heat exchanger, obtained through the results presented individually for the evaporator and condenser, demonstrate that the theoretical model's implementation strategy can contribute to improving the heat exchanger acting locally. For example, the number of fins used on the evaporator need not be the same for the evaporator. **Figures 13** and **14** show theoretical-experimental comparisons for fundamental quantities related to the heat exchanger. The values of the absolute percentage deviations obtained are between 2.0% and 42.1%, with an average deviation equal to 22.5% for effectiveness and 15.9% for the heat transfer rate.

4. Conclusion

The thermal and viscous irreversibility in the heat exchanger, composed of individually finned heat pipes, is analyzed for two air mass flow rates within a borderline range for the air conditioning system, that is, $\dot{m}_{air} = 0.1186\ kg/s$ e $\dot{m}_{air} = 0.1699\ kg/s$. The variables used in the analysis are the number of fins per heat pipe and the number of heat pipes.

The main results obtained through the theoretical analysis were:

- The number of fins per heat pipe and the number of heat pipes significantly affect the value of the Bejan number, and a satisfactory cost-benefit ratio, thermal irreversibility versus total irreversibility, must be sought.
- A compromise between the number of fins and the number of heat pipes with the outlet temperature of the air.
- The highest cost-benefit ratio is associated with the lowest number of fins per heat pipe, equal to 10.
- Considering the air outlet temperature, the number of fins between 10 and 20 for heat pipes equal to 49 for the evaporator and condenser provides a better cost-benefit ratio.
- The values of the absolute percentage deviations obtained are between 2.0% and 42.1%, with an average deviation equal to 22.5% for effectiveness and 15.9% for the heat transfer rate.

The recommended individualized procedure proved consistent and can be used to improve the thermal-hydraulic performance of a finned heat tube heat exchanger. Refining the model and determining the exact number of fins that allow the best cost-benefit ratio is possible in the study under analysis.

Conflict of interest

The author declares no conflict of interest.

Nomenclature

$Asec$	cross-section area, $[m^2]$
Atr	heat transfer area, $[m^2]$
Cp	specific heat, $[\frac{J}{kgK}]$
C	thermal capacity, $[\frac{W}{K}]$
C_{min}	minimum thermal capacity, $[\frac{W}{K}]$

$C^* = \frac{C_{min}}{C_{max}}$

D_h	hydraulic diameter, $[m]$
Fa	fin analogy
h	coefficient of heat convection, $[\frac{W}{m^2K}]$
k	thermal conductivity, $[\frac{W}{mK}]$
K	kelvin
k_W	thermal conductivity of the tube, $[\frac{W}{mK}]$
k_{Fin}	thermal conductivity of the fin, $[\frac{W}{mK}]$
L	vertical or horizontal length, $[m]$
$\dot{m}_{air}$	mass flow rate of the air, $[\frac{kg}{s}]$
N_{Fin}	number of fins
Nu	nusselt number
Pr	prandtl number
$\dot{Q}$	actual heat transfer rate, $[W]$
$\dot{Q}_{max}$	maximum heat transfer rate, $[W]$
Re	reynolds number
T	temperatures, [°C]
Uo	global heat transfer coefficient, $[\frac{W}{m^2K}]$

Subscripts

boil	ebulição
Cd	condenser
Cond	condenser
effect	effective
Ev	evaporator
ext	external
HP	heat pipe
H	horizontal
in	inlet
int	internal
out	outlet
sat	saturation

Greek symbols

α	thermal diffusivity, $[\frac{m^2}{s}]$
β	the relationship between areas
ρ	density of the fluid, $[\frac{kg}{m^3}]$
μ	dynamic viscosity of the fluid, $[\frac{kg}{ms}]$
ν	kinematic viscosity of the cold fluid, $[\frac{m^2}{s}]$

ε_T	thermal effectiveness
η_T	thermal efficiency
ΔT	a difference of temperatures, [°C]

Acronyms

FHPHE	finned heat pipe heat exchanger
Ev	evaporators
Cd	condenser
NHP	number of heat pipes
NFin	number of fins
Nrows	number of rows
NTU	number of thermal units

References

1. Górecki G, Łęcki M, Gutkowski AN, et al. Experimental and numerical study of heat pipe heat exchanger with individually finned heat pipes. *Energies* 2021; 14(17): 5317. doi: 10.3390/en14175317
2. Nogueira E. Localized theoretical analysis of thermal performance of individually finned heat pipe heat exchanger for air conditioning with freon r404a as working fluid. *Materials Science and Chemical Engineering* 2023; 11(8): 61–85. doi: 10.4236/msce.2023.118005
3. Fakheri A. Heat Exchanger Efficiency. *Heat Transfer* 2007; 129(9): 1268–1276. doi: 10.1115/1.2739620
4. Nogueira E. Thermo-hydraulic optimization of shell and externally finned tubes heat exchanger by the thermal efficiency method and second law of thermodynamics. *International Journal of Chemical and Process Engineering Research* 2022; 9(1): 21–41. doi: 10.18488/65.v9i1.3130
5. Nogueira É. Thermal performance in heat exchangers by the irreversibility, effectiveness, and efficiency concepts using nanofluids. *Journal of Engineering Sciences* 2020; 7(2): F1–F7. doi: 10.21272/jes.2020.7(2).f1
6. Putra NSD, Anggoro T, Winarta A. Experimental study of heat pipe heat exchanger in hospital hvac system for energy conservation. *International Journal of Advance Science Engineering Information Technology* 2017; 7(3): 871–877. doi: 10.18517/ijaseit.7.3.2135
7. Höhne T. CFD simulation of a heat pipe using the homogeneous model. *International Journal of Thermofluids* 2022; 15: 100163. doi: 10.1016/j.ijft.2022.100163
8. Jouhara H, Almahmoud S, Brough D, et al. Experimental and theoretical investigation of the performance of an air to water multi-pass heat pipe-based heat exchanger. *Energy* 2021; 219: 119624. doi: 10.1016/j.energy.2020.119624
9. Barrak A. Heat pipes heat exchanger for HVAC applications. In: Vega MA (editor). *Heat Transfer—Design, Experimentation, and Applications*. IntechOpen; 2021.
10. Jouhara H, Chauhan A, Nannou T, et al. Heat pipe-based systems—Advances and applications. *Energy* 2017; 128: 729–754. doi: 10.1016/j.energy.2017.04.028
11. Abd El-Baky MA, Mohamed MM. Heat pipes heat exchanger for heat recovery in air conditioning. *Applied Thermal Engineering* 2007; 27(4): 795–801. doi: 10.1016/j.applthermaleng.2006.10.020
12. Sukarno R, Putra N, Hakim II, et al. Multi-stage heat-pipe heat exchanger for improving energy efficiency of the HVAC system in a hospital operating room. *International Journal of Low-Carbon Technologies* 2021; 16(2): 259–267. doi: 10.1093/ijlct/ctaa048
13. Abedalh AS, Yasin NJ, Ameen HA. Thermal performance of HAVC system using heat pipe heat exchanger. *Journal of Mechanical Engineering Research and Developments* 2021; 44(2): 336–344.
14. Amini A, Miller J, Jouhara H. An investigation into the use of the heat pipe technology in thermal energy storage heat exchangers. *Energy* 2017; 136: 163–172. doi: 10.1016/j.energy.2016.02.089
15. Hakim II, Sukarno R, Putra N. Utilization of u-shaped finned heat pipe heat exchanger in energy-efficient HVAC systems. *Thermal Science and Engineering Progress* 2021; 25: 100984. doi: 10.1016/j.tsep.2021.100984
16. Rohsenow WM. A method of correlating heat transfer data for surface boiling of liquids. *Transactions of the American Society of Mechanical Engineers* 1952; 74(6): 969–975. doi: 10.1115/1.4015984